H-3-4

Extended Abstracts of the 2015 International Conference on Solid State Devices and Materials, Sapporo, 2015, pp924-925

Experimental Demonstration and Modeling of $GeTe_6$ Oscillators and Threshold Switches for Emerging Architectures and Memory

Abhishek A. Sharma*, Yunus E. Kesim*, James A. Bain, Marek Skowronski, Jeffrey A. Weldon
Electrical & Computer Engineering, Carnegie Mellon University, 5000 Forbes Ave., Pittsburgh, PA, USA
E-mail: abhisheksharma@cmu.edu

Abstract: Frequency tunable compact nano-oscillators have attracted significant interest due to their small footprint and low-power operation in emerging neuromorphic architectures where controlling phase or frequency is essential. In this work we demonstrate both oscillatory response and threshold switching in a chalcogenide-based material system – $GeTe_6$. As a threshold switch, this material shows a selectivity of > 10^3 with a peak ON-state current density of > 2.5 MA/cm^2. We use the Van der Pol equation to identify the operating conditions under which oscillatory behavior is seen as opposed to threshold switching. Specifically, by exploring the role of ballast resistor and parallel capacitance, we control the device dynamics, and in turn control the performance metrics of the oscillator and the threshold switch.

1. Introduction

Oscillators with a wide frequency tuning range have attracted great interest due to their applicability in biomedical applications [1] and emerging computing paradigms like neuromorphic computing [2] and phase-based logic [3]. As building blocks of neuromorphic computing, the oscillators generate phase-based information via coupling to its neighbors through synaptic weights. Such neural networks are known as oscillatory neural networks (ONNs). Implementations of ONNs involve the use of dense arrays of voltage controlled oscillators in phase-locked loops (PLLs) [4], which makes their CMOS implementation both area and power inefficient. This has prompted research in understanding emerging oscillatory devices that can be used for implementing these functions efficiently.

Recently, oxide [5] and chalcogenide-based [6] relaxation oscillators have been explored to show excellent frequency tuning and phase coupling. Usually, the failure mechanisms of such oscillators are (1) threshold switching at certain voltage-ballast combinations or (2) permanent change of the structure of the material (forming). Thus, it is important to study the circuit-device interaction that results in either threshold switching (TS) or oscillatory switching (OS) behavior. The same physics that governs oscillatory behavior in these devices can also be harnessed as crossbar memory element selector to reduce the sneak-path problem [7]. In this paper, we will demonstrate, for the first time, low-voltage relaxation oscillations in CMOS BEOL-compatible $GeTe_6$–based ovonic threshold switches (OTS's), which are known to show stable threshold switching [8]. Furthermore, using the Van der Pol model, we identify through simulations, the conditions necessary to differentiate between threshold switching and oscillations. Thus, with the appropriate ballast resistance and supply voltage, we were able to achieve frequency tunable oscillatory behavior or threshold switching with a selectivity of > 10^3 and the peak ON current of > 2.5 MA/cm^2.

2. Device Physics and Modeling

The devices presented in this work are metal-semiconductor-metal (MSM) structures with 20 nm of W as the bottom electrode, 95 nm RF-sputtered amorphous $GeTe_6$ and 20 nm of W as the top electrode, in a crossbar configuration. Device area was 770 nm x 770 nm (Fig. 1).

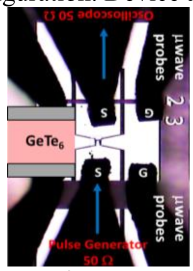

Fig. 1: Stack for $GeTe_6$-based oscillator/threshold switch

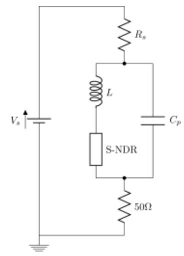

Fig. 2: Circuit schematic of the assumed van der Pol oscillator with a series ballast.

Fig. 2 shows the circuit model that represents our setup and will be used in a Van der Pol (VdP) formalism [9] to model the system behavior. When the supply voltage is increased across the R_S-MSM combination, the voltage across the device also increases until it reaches a certain critical voltage (known as the threshold voltage, V_{th}), as shown in the inset of Fig. 3(a). At V_{th}, the device undergoes a threshold switching process and the resistance of the device changes from high to low. This is attributed to the formation of a temporary conductive filament [5,6]. The nature of the conductive filament is still controversial with both electronic [10] and structural models [6] being invoked to explain its formation. According to field-induced nucleation theory [6], the formation of the filament is due to the nucleation of a super-critical conductive region that later grows, causing it to shunt the field, resulting in the voltage across the device to drop. After this ON-state is reached, if this voltage/current is lower than a certain holding voltage/current (V_h and I_h), the device reverts back to the high resistance state (Fig. 3(b)). If not, the device stays in the ON-state until the supply voltage is reduced so as to cause the device voltage to drop below V_h and I_h. Thus, the device which snaps to a current lower than I_h, will revert back to the OFF state, charge again to V_{th} and cause sustained oscillations (Fig. 3(b)). Similarly, a device that snaps to a value greater than the DC I_h, will stay in the ON-state until the supply voltage pulls it back to OFF state.

When oscillating, device frequency is known to increase by increasing V_S or decreasing R_S [11]. It must be noted that C_p is the aggregate of all parasitic capacitors loading the/threshold switching oscillatory node. The inset shows the same I-V behavior in log scale showing a selectivity of $>10^3$ (Fig. 3(a)) and a peak current density of >2.5 MA/cm^2.

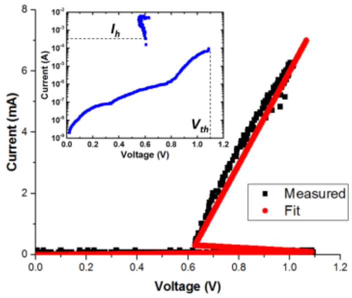

Fig. 3(a): Measured and simulated I-V of the device.

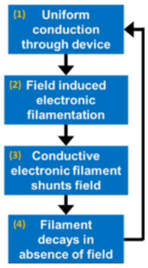

Fig. 3(b): Mechanism of oscillations in the device.

3. Oscillations & Threshold Switching

Fig. 4(a) shows a MSM device undergoing oscillations and threshold switching by increasing the supply voltage from 6 V (OS) to 8 V (TS). Fig. 4(b) represents the schematic increase in the x-intercept of the load-line (representing V_S). If the intercept of the load-line on the device I-V has a negative slope, the device undergoes OS; whereas, if the intersection point is on a positive slope, the device undergoes TS. Thus, an increase in the supply voltage causes the device to exhibit TS behavior, instead of OS. A similar effect can also be achieved with R_S. This helps us define a design space in R_S and V_S that can set peak frequency of oscillations.

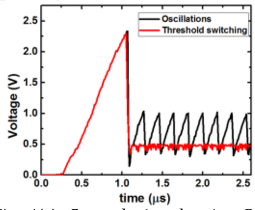

Fig. 4(a): Same device showing OS (black) and TS (red) behavior at V_S of 6 V and 8 V respectively.

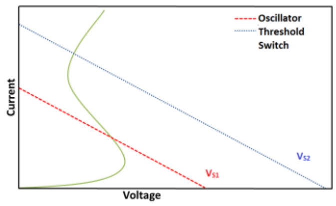

Fig. 4(b): Change in the mode of operation from an oscillatory element and as a threshold switch.

Fig. 5 shows the experimental change in the frequency of oscillations from 300 kHz to 4.5 MHz as a function of R_S. Fig. 6 corroborates this monotonic decrease of frequency with increasing R_S, with a simulated VdP model. Moreover, for the same R_S, increasing V_S causes the device to TS, as indicated in the Fig. 6, following Fig. 4(a), (b).

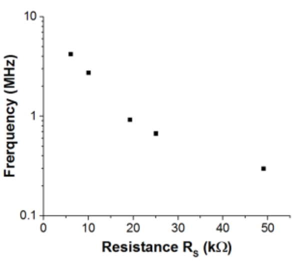

Fig. 5: Device showing oscillatory (black) and threshold switching (red) behavior.

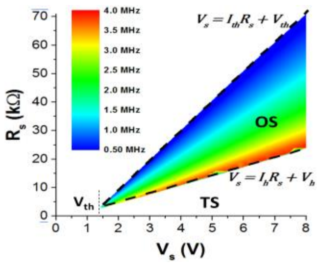

Fig. 6: Change in the frequency of operation in the OS mode, as affected by R_S and V_S.

As expected, Fig. 5 shows the frequency decreasing as the R_S is increased for the same V_S of 6 V. As the frequency is limited by the charging time in the OFF state [11], increasing the capacitance that loads the oscillating node would also decrease the frequency, as previously reported [11]. We see the same effect by adding an external capacitance C, in parallel with the device capacitance, C_P (Fig. 7).

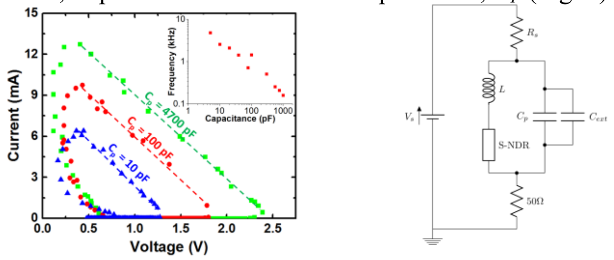

Fig. 7: I-V phase portrait of oscillations, when ballasted with an external capacitor.

The effect of parasitics in the VdP equation has been previously examined with a metric of the ratio of inductance to capacitance, L/C_{TOT} [11], where C_{TOT} is the sum of C_P and C. It is interesting to note that while the oscillation frequency was found to be a function of the series resistance (R_S) and C_{TOT}, the load-line tracing the snap-back from OFF state to ON state has a nearly constant slope (Fig. 7). This slope corresponds to a resistance of ~150 Ω. This resistance appears while the device is transitioning from high to low resistance state; and hence it denotes the discharge path of C_{TOT}. Thus, the discharge takes place from the parasitic capacitor, through the device, a 50 Ω oscilloscope resistance to ground. Thus, ~100 Ω (150 Ω - 50 Ω) can be extracted as the resistance of the filament, consistent with the values reported earlier [10]. This also implies that the peak discharge current flowing through the device will be significantly higher if the capacitance C is high (Fig. 7).

4. Summary and Conclusions

In this work, we have shown for the first time, sustained relaxation oscillations in GeTe$_6$-based devices which have been reported in the past to show threshold switching behavior. Using Van der Pol formulation, we were able to differentiate between its operation as a threshold switch and as an oscillator. The oscillations were found to be frequency tunable from ~300 kHz to 4.5 MHz through a resistive ballast element. It was also observed that ballast resistance (R_S) and the voltage supply (V_S) not only change the frequency of oscillations but also the mode of operation - from an oscillator to a threshold switch (TS). As a TS, the device showed excellent selectivity of $> 10^3$ and a peak current density of > 2.5 MA/cm^2. This peak current density was modulated by an external ballast capacitor. The discharge path that controlled the peak current was found to be limited by the device ON-state resistance, giving significant insight into engineering the peak current density in TS.

References

[1] Choe, K et al., ISSCC, pp.402,403, 2009. [2] Nikonov, D. E., et al., arXiv preprint arXiv:1304.6125 (2013). [3] Roychowdhury, J., arXiv:1410.5016, 2014. [4] Hoppensteadt, F. C., et al., IEEE Trans. on Neur. Netw. 11.3 (2000): 734-738. [5] Shukla, Nikhil, et al., Sci. Rep., 4 (2014). [6] Nardone, M., et al, J. Appl. Phys. 107.5 (2010): 054519. [7] Yang, J. J. et al, Appl. Phys. Lett., 100(11), 113501. [8] Anbarasu, M., et al., Appl. Phys. Lett. 100.14 (2012): 143505. [9] Van der Pol, B. Journal of Science 2.11 (1926): 978-992. [10] Sharma, A. A., et al., Adv. Func. Mat. 24.35 (2014): 5522-5529. [11] Schöll, E. vol. 10, CUP, 2001.